MOLEKUL
eISSN: 2503-0310

Articles
https://doi.org/10.20884/1.jm.2026.21.1.13888

Synthesis, *in Vitro* Studies of Monocarbonyl Curcumin Analog Compounds Against Breast Cancer Cells and Normal Vero Cells, and *In Silico* Studies on Protein Variation

Endang Astuti*, Widya Rahmawati, Rahmawati Sulistya, Ircham Nur Chabib, Tutik Dwi Wahyuningsih, Tri Joko Raharjo, Muhammad Idham Darussalam Mardjan

Department of Chemistry, Faculty of Mathematics and Natural Sciences, Universitas Gadjah Mada, Bulaksumur, Yogyakarta 55281, Indonesia

*Corresponding author email: endangastuti@ugm.ac.id

Received December 07, 2025; **Accepted** January 29, 2026; **Available online** March 20, 2026

ABSTRACT. The research aims to synthesize monocarbonyl analogs of curcumin (MAC) and evaluate their anticancer activity. The synthesis was carried out by sonication method through Claisen-Schmidt condensation reaction using base catalysts, namely potassium hydroxide and sodium hydroxide. Characterization of the compounds was carried out using TLC Scanner, ATR-IR, ^{1}H-NMR, and ^{13}C-NMR. Monocarbonyl analog of curcumin compounds A, B, and C have been successfully synthesized with purity of 91.13; 95.82; and 87.57%, respectively. The resulting compounds are yellow solids and have good yields. The monocarbonyl analog of curcumin compounds were then tested for cytotoxicity against breast cancer cells (T47D, MCF-7, and 4T1) and normal cells (Vero). Pharmacokinetic prediction and toxicity (ADMET) was performed using an online site (pkCSM). Monocarbonyl analogs of curcumin compounds were predicted to have a better pharmacokinetic profile compared to curcumin. Molecular docking was carried out using Autodock Vina to determine the interaction of curcumin and monocarbonyl curcumin analog compounds with EGFR, Bcl-2, and p53 mutants. Based on molecular docking, the proposed monocarbonyl analogs of curcumin generally exhibit lower binding affinities that curcumin and form specific interactions with amino acid residues inf target proteins.

Keywords: Claisen-Schmidt condensation, molecular docking, monocarbonyl analog of curcumin.

INTRODUCTION

Cancer is a complex sequence of disease conditions that progresses gradually, with a generalized loss of growth control (Debela et al., 2021). Breast cancer is a multifactorial disease triggered by genetic changes that promote tumor growth and progression (Hassan et al., 2024). Breast cancer treatment includes surgery, chemotherapy, radiotherapy, endocrine therapy, targeted therapy, and immunotherapy (Wang & Wu, 2023). The most common effects of breast cancer treatment are pain, infections, hair loss, and tissues impairment. Moreover, cancer cells can develop resistance to antitumor drugs over time (Pourmadadi et al., 2023).

Currently, the development of breast cancer drugs is still progressing. One of the components in medicinal plants that is widely researched for cancer treatment is curcumin. Curcumin has various biological activities, including antioxidants, antimicrobial, anti-inflammatory, antidiabetic, and anticancer (Sohn et al., 2021). Curcumin has shown anticancer effects against various cancers, such as breast, liver, lung, stomach, and prostate (Yang et al., 2022). Despite the diverse biological activities of curcumin, it has limitations such as low water solubility, poor oral absorption, and rapid metabolism and excretion, leading to low bioavailability of curcumin in the body. This limits the clinical applications of curcumin (Jamil et al., 2023). Modification of curcumin into curcumin analogs has been carried out and is reported to improve its pharmacokinetic properties, bioavailability, and biological activity (Kaur et al., 2024). Curcumin can be modified into curcumin analogs by replacing the β-diketone group with monocarbonyl (Zelelew et al., 2023). Curcumin analogs can be synthesized using the Claisen-Schmidt condensation reaction with aldehyde and ketone reactants. This reaction is commonly used because it is simple (Eryanti et al., 2015). Mustika et al. (2024) also reported that the synthesis of curcumin analogs from aldehyde derivatives and N-benzylpiperidin-4-one, using NaOH as the base catalyst and stirring, was successfully carried out, yielding compounds in 71% yield.

In the discovery and development of new drugs, in silico test is an important part to be performed. Molecular docking is one of the in silico tests which facilitates the prediction of preferred binding orientation of one molecule (ligand) to another molecule (receptor), when both interact each other in

order to form a stable complex (Agarwal & Mehrotra, 2016).

Molecular docking of curcumin analogs was performed against epidermal growth factor receptor (EGFR), B-cell lymphoma-2 (Bcl-2), and tumor suppressor gene p53 (p53) proteins that play important roles in cancer cell proliferation and apoptosis pathways. Therefore, we initially synthesized three curcumin analogs through the Claisen-Schmidt condensation and performed molecular docking against the proteins of EGFR, Bcl-2, and p53 mutants. All synthesized compounds were evaluated for their cytotoxic activity against breast cancer cells lines, such as T47D, MCF-7, 4T1, and normal cells (Vero). The evaluation of pharmacokinetic properties and toxicity (ADMET) was also carried out.

EXPERIMENTAL SECTION

The monocarbonyl analogs of curcumin used for molecular docking study were (3*E*,5*E*)-1-benzyl-3,5-bis((*E*)-3-phenylallylidene)piperidin-4-one (1), (3*E*,5*E*)-3,5-bis(2- hydroxybenzylidene)-1-methylpiperidin-4-one (2), and (3*E*,5*E*)-1-benzyl-3,5-bis(2- hydroxybenzylidene)piperidinia one (3).

The materials used for the synthesized monocarbonyl analogs of curcumin included cinnamaldehyde, 2-hydroxybenzaldehyde, potassium hydroxide, ethanol, methanol, chloroform, ethyl acetate, n-hexane, dimethyl sulfoxide, dichloromethane, silica gel GF254, and TLC silica gel 60 F254 from Merck. *N*-benzylpiperidin-4-one, *N*-methylpiperidin-4-one from Chemie. IDN, and hydrochloric acid from Mallinckrodt.

For the *in vitro* cytotoxicity assay breast cancer cells (T47D, MCF-7, and 4T1), normal cell (Vero) from parasitology laboratory of FKKMK-UGM, 96-well plate, Roswell Park Memorial Institute 1640 (RPMI), 3-(4,5-dimethyl thiazol-2yl)-2,5-diphenyl tetrazolium bromide (MTT), Dulbecco's Modified Eagle Medium (DMEM), trypsin-EDTA 0.25%, Fetal Bovine Serum (FBS), Phosphate Buffer Saline (PBS), penstrep (Penicillin- Streptomycin) 2%, sodium dodecyl sulphate (SDS), and hydrochloric acid (HCl) 0.01 N.

The compounds were reacted in a sonicator (Power Sonic 505) and monitored via TLC under UV light at 245 nm. Purity was measured using a TLC Scanner (CAMAG) and the melting point was determined using an electrothermal (IA9100). ATR-IR spectra were recorded using Shimadzu® IRTracer-100 spectrometer. ^{1}H-NMR and ^{13}C-NMR spectra were measured on a JEOL JNMECA spectrometer at 500 MHz and 125 MHz, respectively.

Synthesis Procedure

Synthesis of (3E,5E)-1-benzyl-3,5-bis((E)-3-phenylallylidene)piperidin-4-one (1)

Compound 1 was synthesized from 3.70 mmol of cinnamaldehyde and 1.85 mmol of *N*-benzyl-4-piperidone in 10 mL of ethanol. The mixture was stirred at room temperature for 20 minutes, followed by the dropwise addition of 2 mL of 10% KOH. The mixture was then sonicated at 52 °C for 95 minutes. The reaction product was washed with distilled water:acetone (1:1), filtered, and dried. The product was then filtered and subsequently dried. The purity of the compound was determined by melting point analysis and TLC scanning using an *n*-hexane : ethyl acetate (8:2) eluent.

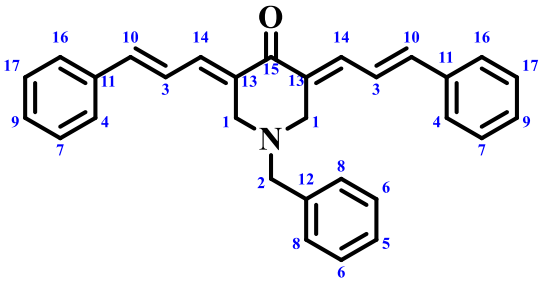

(1)

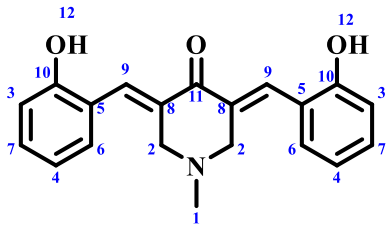

(2)

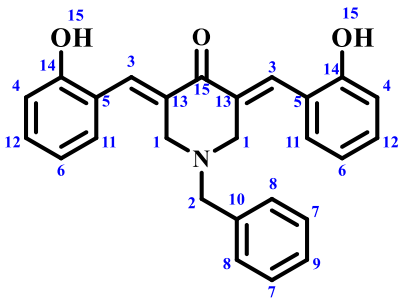

(3)

Figure 1. Chemical structures of curcumin analogs (1-3)

Molecular formula $C_{30}H_{27}NO$, yellow solid (40.15% yield), m.p. 148.3-150.8 °C, purity: 91.13%. ATR-IR ν (cm^{-1}): 3016, 1659, 1582, 1552, 1447, 1296. ^{1}H-NMR ($CDCl_3$) δ (ppm): 7.46 (t, *J*=9 Hz, 6H, Ar–H), 7.27-7.40 (m, 12H, Ar–H), 6.99 (d, *J*=15.3 Hz, 2H, CH=C, C_{10}), 6.84 (dd, *J* =11.7 Hz; 15.3 Hz, 2H, C=CH–C, C_3), 3.79 (s, 2H, N–CH_2–Ar, C_2), 3.75 (s, 4H, C–CH_2–N, C_1). ^{13}C-NMR ($CDCl_3$) δ (ppm): 186.74 (C=O, C_{15}), 145.71 (Ar–CH=C, C_{14}), 137.71 (–C=C–, C_{13}), 136.82 (C_{Ar}), 135.15 (C_{Ar}), 132.59 (Ar–CH=C, C_{10}), 129.48 (C_{Ar}), 129.39 (C_{Ar}), 128.91 (C_{Ar}), 127.84 (C_{Ar}), 127.69 (C_{Ar}), 122.8 (–C=C–, C_3), 61.19 (N–CH_2–Ar, C_2), 52.65 (CH_2, C_1).

Synthesis of (3E,5E)-3,5-bis(2-hydroxybenzylidene)-1-methylpiperidin-4-one (2)

Compound **2** was synthesized from 4 mmol of 4-hydroxybenzaldehyde and 2 mmol of *N*-methylpiperidin-4-one in 5 mL of ethanol. The mixture was stirred at room temperature for 30 minutes, followed by the dropwise addition of 5 mL of 40% NaOH. The mixture was then sonicated at room temperature for 6 hours. The mixture was then neutralized with HCl and cold distilled water. The product was then filtered and subsequently dried. The product was purified using preparative TLC with ethyl acetate and *n*-hexane eluent. The purity of the compound was determined through by melting point analysis and TLC scanning using an ethyl acetate:methanol (3:2) eluent.

Molecular formula $C_{20}H_{19}NO_3$, yellow solid (85.57 % yield), m.p. 136.5-139.2 °C, purity: 100%. ATR-IR ν (cm^{-1}): 3387, 1651, 1589, 1450, 1249, 1112, 748. ^{1}H-NMR (DMSO) δ (ppm): 7.32 (dd, *J*=7.5, 1.7 Hz, 2H, Ar-H, C_6), 7.16 (td, *J*=7.7, 1.7 Hz, 2H, Ar-H, C_7), 7.01 (td, *J*=7.5, 1.2 Hz, 2H, Ar-H, C_4), 6.89 (s, 4H, OH, CH, C_9), 6.76 (d, *J*=8.1 Hz, 2H, Ar-H, C_3), 3.40 (d, *J*= 13.3 Hz, 2H, CH_2, C_{2b}), 3.23 (dd, *J*=13.2, 1.8 Hz, 2H, CH_2, C_{2a}), 2.22 (s, 3H, CH_3, C_1). ^{13}C-NMR (DMSO) δ (ppm): 150.29 (C=O, C_{11}), 130.05 (C-OH, C_{10}), 127.62 (C=C, C_9), 127.49 (C=C, C_8), 123.91 (C_{Ar}, C_7), 122.79 (C_{Ar}, C_6) 121.71 (C_{Ar}, C_5), 116.89 (C_{Ar}, C_4), 94.61 (C_{Ar},C_3) 53.77 (CH_2, C_2), 45.04 (CH_3, C_1).

Synthesis of (3E,5E)-1-benzyl-3,5-bis(2-hydroxybenzylidene)piperidin-4-one (3)

Compound **3** was synthesized from 4 mmol of 4-hydroxybenzaldehyde and **2** mmol of *N*-benzylpiperidin-4-one in 5 mL of ethanol. The mixture was stirred at room temperature for 30 minutes, followed by the dropwise addition of 1.2 mL of 40% NaOH. The mixture was then sonicated at room temperature for 6 hours. The mixture was then neutralized with HCl and cold distilled water. The product was then filtered and subsequently dried. The product was purified by preparative TLC using ethyl acetate : *n*-hexane eluent. The purity of the compound was determined through the melting point analysis and TLC scanner with *n*-hexane:ethyl acetate (1:3) eluent.

Molecular formula $C_{26}H_{23}NO_3$, orange solid (92.50% yield), m.p. 141.9-144.2 °C, purity: 100%. ATR-IR ν (cm^{-1}): 3279, 3032, 1658, 1604, 1481, 1219, 941, 748. ^{1}H-NMR ($CDCl_3$) δ (ppm): 3.51 (2, 4H, CH_2, C_1), 3.68 (s, 2H, CHPh, C_2), 6.76 (s, 2H, CH, C_3), 7.03 (d, *J*=8.0 Hz, 2H, CH_{Ar}), 7.19 (t, *J*=7.5 Hz, CH_{Ar}), 7.31 (m, 9H, CH_{Ar}, CHPh, OH (C_{15})). ^{13}C-NMR ($CDCl_3$) δ (ppm): 52.10 (CH_2, C_1), 61.44 (CH_2, C_2), 94.93 (CH, C_3), 117.06 (CH_{Ar}, C_4), 121.36 (C_{Ar}, C_5), 122.27 (CH_{Ar}, C_6), 124.22 (CHPh, C_7), 126.96 (CHPh, C_8), 127.27 (CHPh, C_9), 127.45 (CPh, C_{10}), 128.59 (CH_{Ar}, C_{11}), 129.26 (CH_{Ar}, C_{12}), 129.63 (C, C_{13}), 138.49 (C-OH, C_{14}), 150.46 (C=O, C_{15}).

Molecular Docking Study

Following optimization and docking methods as reported in Oubahmane et al. 2023, compounds **1-3** were modelled using ChemDraw Ultra 12.0 and optimized with Gaussian 09W (Frisch et al., 2016) using the semi-empirical AM1 (Dewar et al., 1985) method. The protein structures were obtained from the Protein Data Bank (PDB), including EGFR (ID: 1M17), Bcl-2 (ID: 6O0K), and p53 mutant (ID: 2X0W). Proteins and native ligands were separated and optimized using AutoDockTools 1.5.6. Docking simulations were performed using AutoDock Vina (Trot and Olson, 2009). The grid box sizes used were 20 x 20 x 20 Å with 1.000 Å spacing. The most suitable conformation was selected based on the lowest binding affinity and the interactions with the ligand's active site. The visualization of the docking results was carried out using Discovery Studio Visualizer (DSV) 2017.

In Vitro Cytotoxicity Test against Breast Cancer Cells and Normal Cells

Cytotoxicity assays against breast cancer cell lines (T47D, MCF-7, and 4T1) and a normal cell line (Vero) were performed using the MTT assay, following the standard protocol of the Cancer Chemoprevention Research Center – Universitas Gadjah Mada (CCRC UGM, 2009). T47D cells were seeded into RPMI medium, and MCF-7, 4T1, and Vero were seeded into DMEM medium at a density of 10,000 cells/well and incubated for 24 hours at 37 °C with 5% CO_2. Each compound was dissolved in DMSO and RPMI/DMEM medium to obtain final concentrations of 100, 50, 25, 12.5, and 6.25 μg /ml. Following incubation, the cells were treated with 100 μL of the prepared test samples. The plates were incubated under the same conditions for an additional 24 hours. Subsequently, 100 μL of MTT reagent was added to each well, and the cells were incubated for 4 hours. Then, 100 μL of 10% SDS-HCl stopper solution was added to each well. The method was performed in triplicate. Absorbance was measured at 595 nm using an ELISA reader, and the resulting data were used to calculate the IC50 values for each sample. Following the IC_{50} value, the

selectivity index (SI) was calculated using Equation 1.

Selectivity index (SI) $= \frac{IC_{50\ (\text{normal cell})}}{IC_{50\ (\text{cancerous cell})}}$. (Equation 1)

Prediction Pharmacokinetic Profile and Toxicity

The physicochemical and pharmacokinetic (ADMET) parameters were predicted using the pkCSM web server by entering the SMILES list of curcumin analogs.

RESULTS AND DISCUSSION

Synthesis of Monocarbonyl Analog of Curcumin

Compounds 1, 2, and 3 were carried out via Claisen-Schmidt condensation (Figure 2). Compound 1 was prepared by reacting cinnamaldehyde with *N*-benzylpiperidin-4-one using ethanol as solvent and 10% KOH as catalyst. Compound 2 was synthesized via the reaction of 2-hydroxybenzaldehyde and *N*-methylpiperidin-4-one, whereas compound 3 was synthesized from *N*-benzylpiperidin-4-one under ethanolic conditions. Both compounds were synthesized using ethanol a solvent and 40% NaOH as a catalyst. The synthesis product was obtained in good yield.

Based on the analysis of the NMR spectra, the synthesis of monocarbonyl curcumin analog was confirmed successful by the presence of one singlet at 6.76 and 6.89 ppm for compound 2 and 3 representing the alkene. In compound 1, the double bond was indicated by a multiplet signal observed at 7.23-7.41 ppm. The ATR-IR spectrum also confirmed the formation of curcumin analog by the appearance of absorption band at 1658 cm^{-1} representing the conjugated C=O group. On the other hand, the absorption band at 748 cm^{-1} corresponded to the subtitution ortho of OH group. In addition, the absorption band at 1219, 1249, and 1296 cm^{-1} was indicated as C-N aliphatic stretching.

Molecular Docking Study

Molecular docking aims to computationally simulate molecular process and optimize the conformation of both ligands and proteins. In this study, EGFR, Bcl-2, and p53 mutants were selected as receptors due to their overexpression in breast cancer cells, making them great potential as therapeutic targets. Before performing docking, method validation was conducted by redocking the native ligand to the target protein. The parameter used for redocking evaluation is the RMSD (Root Mean Square Deviation) value. The RMSD value describes how much the ligand-receptor conformation changes between the initial and the ligand-receptor conformation after redocking. The method is considered valid if the RMSD is ≤ 2 Å, thereby allowing its use for molecular docking of new compounds (Muttaqin et al., 2019). Table 1 presents the molecular docking results of three curcumin analogs and curcumin, used as a reference ligand, against three target receptors.

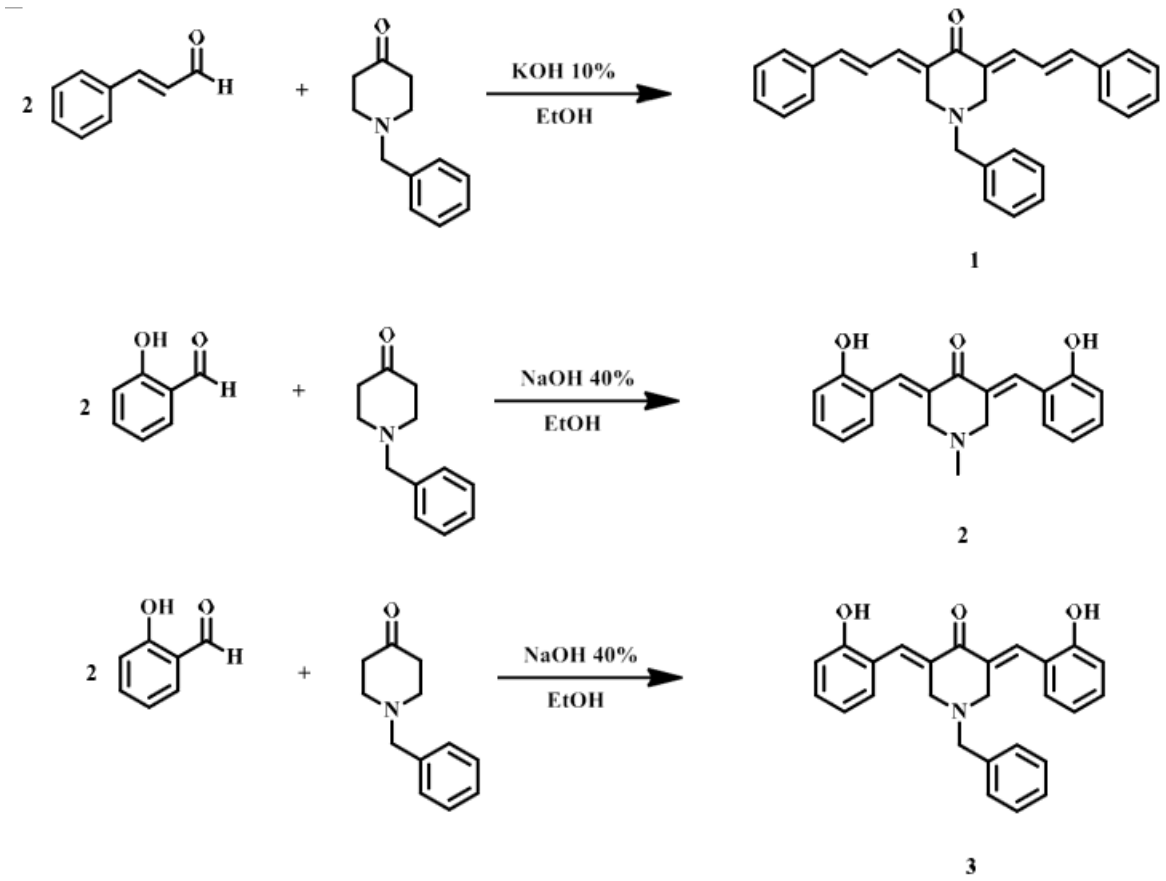

Figure 2. Synthesis of compound 1, 2, and 3 via Claisen-Schmidt condensation

Table 1. Molecular docking result of compound **1-3** against EGFR, Bcl-2, and p53 mutants

Receptor targets	Ligands	Binding Affinity (kcal/mol)	Interactions
EGFR	Erlotinib (Native ligand)	-7.0	H-bond: **Met769** Hydrophobic: Leu694, Val702,Ala719, **Lys721**, Met742, Leu764, Gln767, Pro770, Leu820, Thr830 Van der Waals: Gly695, Phe 699, Glu738, Leu753, Thr766, Leu768, Phe771, Gly772, Asp831
	1	-9.6	H-bond: **Met769** Hydrophobic: Val702, Leu820, **Lys721**, Thr766 Van der Waals: Gly695, Phe699, Asp831, Glu738,Met742, Leu764, Ala719, Leu768, Leu694, Gly772, Cys773
	2	-8.6	H-bond: **Met769** Hydrophobic: Leu694, Val702, Ala719, **Lys721**, Met742, Leu764, Gln767, Gly772, Leu820, Thr830 Van der Waals: Glu738, Leu753, Thr766, Leu768, Pro770, Val702, Cys773, Asp831
	3	-9.4	H-bond: **Met769**, Asp831 Hydrophobic: Leu694, Val702, **Lys721**, Thr830 Van der Waals: Phe699, Ala719, Glu738, Pro770, Phe771, Gly772, Thr766, Leu768, Met742, Leu820, Arg817
	Curcumin	-7.6	H-bond: **Met769**, Cys751 Hydrophobic Phe699, Val702, Ala719, **Lys721**, Glu738, Met742, Thr766, Asp831 Van der Waals: Leu694, Leu764, Gly772 Leu768, Leu820, Thr830, Phe832
Bcl-2	Venetoclax (Native ligand)	-11.1	H-bond: Arg107, **Gly145**, Tyr202 Hydrophobic: Phe104, Tyr108, Phe112, Met115, Val133, Leu137, Arg146, Ala149, Val156 Van der Waals: Ala100, Ser105, Asp108, Asp111, Glu136, Asn143, Trp144, Val148, Glu152, Phe158, Phe198
	1	-9,0	H-bond: Tyr108 Hydrophobic: Phe104, Ala149, Gly145, Val148, Tyr202, Ala100, Arg107 Van der Waals: Asp111, Phe198, Asp103, Leu137
	2	-6.5	H-bond: Gly145, Tyr 202 Hydrophobic: Ala100, Asp103, Trp144 Van der Waals: Phe104, Asn143, Val148
	3	-9.0	H-bond: Gly145 Hydrophobic: Phe104,Tyr108, Val133, Ala149 Van der Waals: Asp111, Phe112, Met115, Leu137, Glu136, Arg146, Phe153
	Curcumin	-7.0	H-bond: Ala100, Gly145, Tyr202 Hydrophobic: Asp103, Phe104, Trp144 Van der Waals: Arg107, Tyr108, Asn143, Val148
p53 mutant	X0W (Native ligand)	-5.0	H-bond: Thr150 Hydrophobic: Val147, Pro151, Glu221, Pro222, Pro223 Van der Waals: Thr155, Leu145, Cys220, Thr230, Leu257
	1	-6,3	H-bond: Thr150 Hydrophobic: Trp146, Thr230, Pro223, Leu145, Val147, Cys220, Leu257, Pro151, Pro222, Pro153 Van der Waals: Asp228, Cys229, Phe109, Pro152, Gly154, Thr155, Glu221, Arg110
	2	-5.5	H-bond: Thr150 Hydrophobic: Pro151, Cys220, Glu221, Pro222, Pro223, Van der Waals: Val147, Thr230
	3	-6.1	H-bond: Asp148, Thr150 Hydrophobic: Val147, Pro223, Asp228 Van der Waals: Arg110, Trp146, Pro151, Pro222, Cys229, Thr230
	Curcumin	-5.3	H-bond: Thr150 Hydrophobic: Val147, Pro151, Pro153, Glu221, Pro222, Pro223 Van der Waals: Gly154, Thr155, Cys220, Thr230

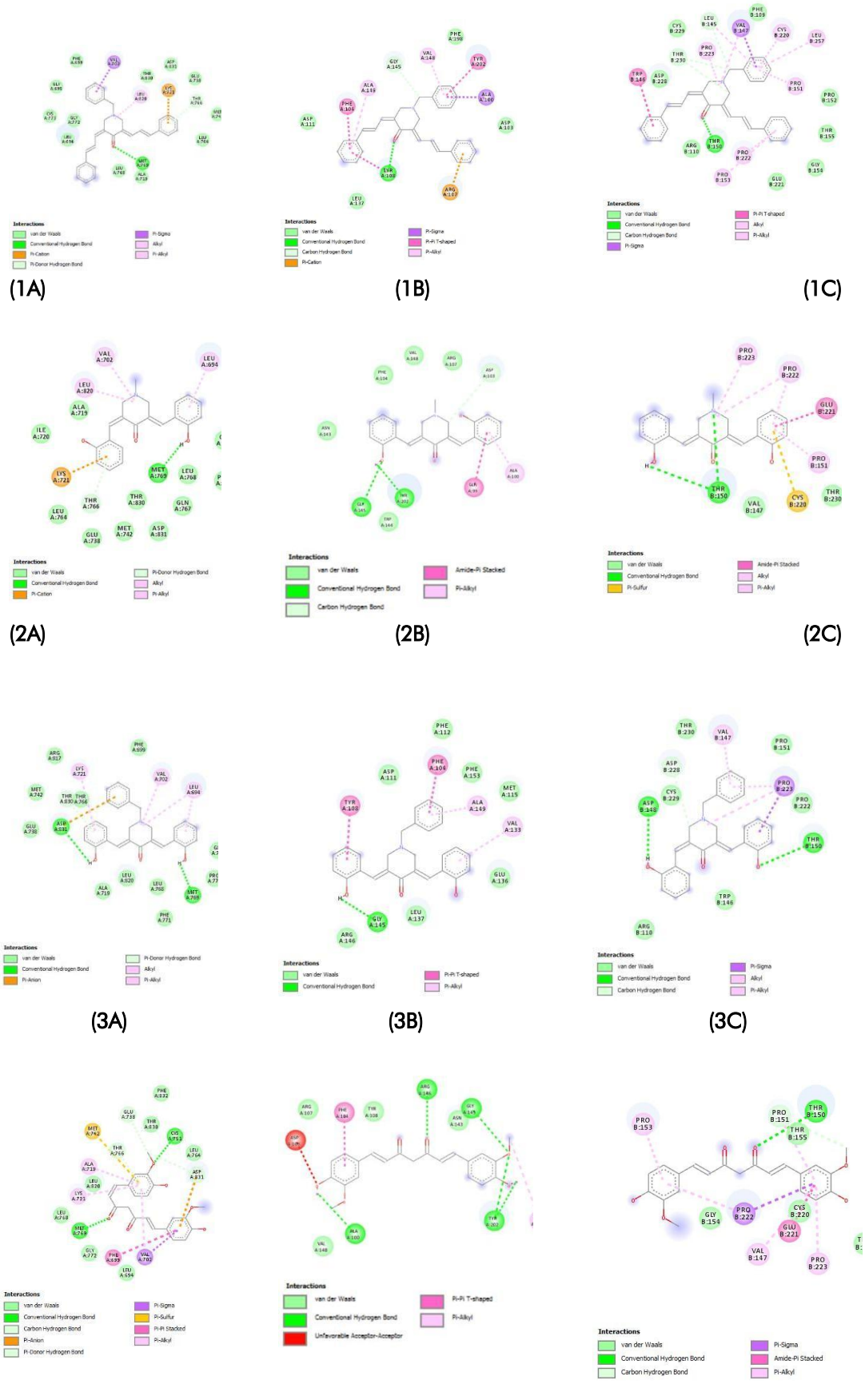

Figure 3. The visualization of interactions between compound **1**, **2**, **3**, and curcumin against: (**A**) EGFR, (**B**) Bcl-2, (**C**) p53 mutants

Molecular docking results indicated that all compounds had lower binding affinity compared to the native ligand and curcumin for the EGFR and p53 mutant proteins. Although all compounds generally exhibited lower binding affinity values than curcumin for the Bcl-2 protein, they were not superior to the native ligand. Furthermore, all monocarbonyl curcumin analogs exhibited specific interactions with the active sites of the target proteins.

Key amino acid residues in the active site of the EGFR protein are Met769 and Lys721 (Fathima, 2024). Compounds **1-3** primarily interact via conventional hydrogen bonding with Met769 residue. Adeniyi et al. (2022) reported that the active side of Bcl-2 protein is found at amino acid residue Gly145 for hydrogen bonding and other interactions with amino acid residues Phe104, Arg146, Tyr108, Leu137, Glu136, Met115, and Asp111. Compounds **2** and **3** primarily interact via conventional hydrogen bonding with Gly145 residue, except for compound **1**, which forms a hydrogen bond with the Tyr108 residue. Malki et al. (2017) performed molecular docking on the mutant p53 protein, which showed interactions involving amino acid residues, including hydrogen bonds at Thr150 and hydrophobic interaction at Val147, Pro151, Cys220, and Glu221. Compounds **1-3** primarily interact via conventional hydrogen bonding with Thr150 residue. The visualization of the interactions between the three curcumin analogs against three target receptors was presented in **Figure 3.**

In Vitro Cytotoxicity Assay

The cytotoxicity assay on breast cancer cells and normal cell was performed using MTT method with results reported as IC50 values, which indicate the concentration required to inhibit 50% of the cell population. The sample used in this assay included compounds **1**, **2**, and **3**, along with curcumin as comparative control. The results of the cytotoxicity assay are summarized in **Table 2.**

A compound is classified as exhibiting strong cytotoxicity if the IC50 value is less than 20 µg/mL; moderate cytotoxicity if the IC50 ranges from 20-100 µg/mL; and weak cytotoxicity if the IC50 value exceeds 100 µg/mL (Fikroh et al., 2023). Based on the results obtained, the IC50 values of curcumin were classified as moderate cytotoxicity on T47D, MCF-7, and 4T1 but strong cytotoxicity on Vero. Compound 1 was classified as weakly toxic against T47D, MCF-7, 4T1, and Vero. Compound **2** was classified as strongly toxic on T47D and 4T1 but moderate toxicity on MCF-7 and Vero. Compound **3** was classified as strongly toxic on MCF-7 and 4T1 but moderate toxicity on T47D and weak toxicity on Vero. Based on the results obtained, compounds **2** and **3** has IC50 value less than curcumin although compound **3** for T47D and compound **2** for MCF-7 have a higher IC50 value than curcumin. On the other hand, compound **1** is less toxic than curcumin in all cell types. A compound is classified as exhibiting high selectivity if the value of the selectivity index exceeds 6; moderate selectivity if the value of the selectivity index is between **3-6**; low selectivity if the value of the selectivity index ranges from **1-3**; and not selective if the value of the selectivity index is less than 1 (Sancha et al., 2023). Based on **Table 2**, compound 1 was classified as high selectivity on MCF-7 and 4T1 cell lines, compound **2** was classified as moderate selectivity on 4T1 cell line, compound **3** was classified as high selectivity on T47D, MCF-7, and 4T1 cell lines, and curcumin was classified as less selectivity on all cell lines. These results mean the modification of the diketone group to monocarbonyl in curcumin can increase its bioavailability.

Prediction of Pharmacokinetic Properties and Toxicity

The physicochemical and pharmacokinetic properties, including absorption, distribution, metabolism, excretion, and toxicity were predicted using the pkCSM webserver. The *in silico* prediction of physicochemical and pharmacokinetic properties for all curcumin analogs and curcumin has been shown in **Table 3.**

The physicochemical properties of curcumin analogs and curcumin were analyzed on the basis of Lipinski's Rule of Five. Lipinski et al. (2001) explained that a drug compound which can be taken orally must meet several requirements: a molecular weight < 500 Da; the number of hydrogen acceptors (HBA) ≤ 10; the number of hydrogen bond donors (HBD) ≤ 5; and LogP < 5. Based on **Table 3**, the curcumin analogs have molecular weights ranging from 321.376 to 17.552 g/mol, the number of HBA ranges from 2 to 4, the number of HBD ranges from 0 to 2 and the logP value range from 3.07 to 6.35. Therefore, the analogs **2** and **3** met all the physicochemical parameters, whereas analog **1** did not met the logP parameter.

Table 2. The results of the cytotoxicity assay against breast cancer cells and normal cell

Compound	IC50 (µg/mL)				Selectivity Index (SI)		
	T47D	MCF-7	4T1	Vero	T47D	MCF-7	4T1
Compound **1**	153,240.92	1,241.32	445.47	45,422.94	0.30	36.59	101.97
Compound **2**	21.37	58.33	12.25	59.68	2.79	1.02	4.87
Compound **3**	55.91	18.61	18.03	3,125.07	55.89	167.92	173.33
Curcumin	22.12	28.19	22.12	16.23	0.73	0.58	0.73

Table 3. The results of the prediction of pharmacokinetic properties and toxicity

Parameters	Compound			
	1	**2**	**3**	**Curcumin**
Lipinski's rule				
Molecular weight <500Da	417.552	321.376	397.474	368.385
nHA <10	2	4	4	6
nHD <5	0	2	2	2
logP <5	6.35	3.0793	4.6497	3.3699
(A) Absorption				
Water Solubility	-4.513	-3.504	-4.421	-4.01
Caco2 permeability (log cm/s)	1.093	1.271	0.769	-0.093
Human intestinal absorption (HIA) (%)	92.607	95.314	86.868	82.19
Skin permeability (cm/s)	-2.791	-2.742	-2.768	-2.764
(D) Distribution				
Volume distribution (L/kg)	0.943	0.999	0.63	-0.215
BBB (Log BB)	0.677	-0.47	-0.168	-0.562
(M) Metabolism				
CYP2D6 substrate	Yes	No	Yes	No
CYP3A4 substrate	Yes	No	Yes	Yes
CYP2D6 inhibitor	Yes	No	Yes	No
CYP3A4 inhibitor	No	No	No	Yes
CYP1A2 inhibitor	No	Yes	Yes	Yes
CYP2C9 inhibitor	No	No	No	Yes
CYP2C19 inhibitor	No	No	Yes	Yes
(E) Excretion				
Total clearance (mL/min/kg)	6.601	15.455	14.334	12.800
(T) Toxicity				
AMES mutagenesis	No	Yes	Yes	No
Hepatotoxicity	Yes	No	No	No
oral rat acute toxicity (mg/kg)	2.686	2.413	2.345	1.833

The drug absorption process can be predicted using several parameters, including membrane permeability (indicated by Caco-2 colon cell lines), human intestinal absorption (HIA), and skin permeability. A compound will be considered to have high Caco-2 permeability if its has log Papp > 0.90 cm/s (Azzam, 2023). Analogs **1** and **2** were predicted to have high Caco-2 permeability, however analog 3 and curcumin had low Caco- 2 permeability. In the case of human intestinal absorption, an absorption value of higher than 70% is considered to be well absorbed (Radchenko et al., 2016). All analogs predected had better HIA values and good absorption than curcumin. A molecule will be considered to have excellent skin permeability if the permeability coefficient (Papp) is more than 2×10^{-6} cm/s. The prediction showed that all curcumin analogs had good skin permeability. The solubility characteristic of the compounds is defined as insoluble if more negative than -10. The values of the poorly soluble compounds ranged between -10 and - 6. The higher than -6 and less than -4 is classified as moderately soluble. The soluble compounds are in between -4 and -2. The values between -2 and 0 are very soluble, while higher than zero are highly soluble (Mvondo et al., 2021). The solubility values from the **Table 3** reveal that analog 2 is very soluble. Analogs **1** and **3** are predicted moderately soluble.

The distribution of a compound described by the distribution volume (VD) and the blood-brain barrier

membrane permeability (log BB). The distribution volume is a parameter used to calculate the volume in which the entire quantity of a drug is distributed at a uniform concentration in blood plasma. A compound will be assumed to have a proper VD if it has a VD value in the range of 0.04 – 20.00 L/kg (Firdausy et al., 2020). Based on **Table 3**, the volume of distribution of all curcumin analogs was categorized as good. The blood-brain barrier (BBB) is a parameter to determining a drug's ability to cross the blood-brain. A compound will easily cross the brain when the log BBB is higher than 0.3 (Pratama et al., 2020). The analog **1** was predicted to readily cross the blood-brain barrier, whereas analogs **2** and **3** might moderately penetrate the blood-brain barrier.

Cytochrome 450 is an enzyme that contributes to the detoxification of foreign chemicals and the metabolism of drugs. There are five CYP450 enzymes that metabolize 90% of drugs, namely CYP1A2, CYP2C9, CYP2C19, CYP2D6, and CYP3A4 (Al Sheikh Ali et al., 2021). As displayed in **Table 3**, compound **1** and **3** was the substrate for CYP2D6 and CYP3A4, compound **2** was not a substrate for CYP2D6 and CYP3A4, and curcumin was not a substrate for CYP2D6 but was a substrate for CYP3A4. Additionally, compound **1** was predicted to inhibit CYP2D6, compound **2** was predicted to inhibit CYP1A2, compound **3** was predicted to inhibit CYP2D6 and CYP1A2, and curcumin was predicted to inhibit CYP1A2, CYP2C9, CYP2C19, and CYP3A4. The prediction suggested that compound **3** may be metabolized in the liver. Curcumin might act as both a substrate and inhibitor of most CYP450 enzymes, indicating that curcumin might be metabolized in the liver.

The excretion parameter was evaluated by predicting the clearance rate (Cl). The higher the Cl value of a compound, the higher the Cl value of a compound, the faster the compound is removed from the body. The prediction showed that the total clearance of compounds **2** and **3** was higher than that of curcumin, indicating that the compounds were eliminated more rapidly from the body.

The potential toxicity of a compound can be predicted from acute oral toxicity (LD50). From **Table 3**, all compounds had LD50 values ranging from 2.345 to 2.686 mg/kg, which seems to be sufficiently safe. The Ames assay is a method used to predict the mutagenic potential of a compound. In this context, compounds **2** and **3** were predicted to be mutagenic. Hepatotoxicity testing is used to predict whether chemicals might induce liver damage. The prediction indicated that only compound **1** might induce hepatotoxicity.

CONCLUSIONS

Compounds **1–3** were identified through molecular docking as candidates with favorable interactions at the active sites of EGFR, Bcl-2, and p53 active sites and were synthesized via Claisen–Schmidt condensation. Modification of the curcumin diketone moiety to a monocarbonyl framework enhanced biological activity. Among the synthesized compounds, compounds **2** and **3** showed significantly improved cytotoxicity against MCF-7 and 4T1 cells. This activity was consistent with molecular docking results, in which compound **3** exhibited stronger EGFR binding than curcumin and formed a stable hydrogen bond with Met769. Pharmacokinetic predictions further supported the drug-likeness and permeability of compound **3**. Overall, compound **3** demonstrated the most favorable integrated profile, highlighting its potential as a lead anticancer candidate.

REFERENCES

Adeniyi, A.A., Adeniyi, J.N., Nlooto, M., & Singh, P. (2022). Probing new antileukemia agents that target FLT3 and BCL-2 from traditional concoctions through a combination of mass spectrometry analysis and consensus docking methods. *Applied Science*, *12*, 1-14.

Agarwal, S., & Mehrotra, R. (2016). An overview of Molecular Docking. *JSM Chemistry*, *4*(2), 1-4.

Al Sheikh Ali, A., Khan, D., Naqvi, A., Al-Blewi, F.F., Rezki, N., Aouad, M.R., & Hagar, M. (2021). Design, synthesis, molecular modeling, anticancer studies, and density functional theory calculations of 4-(1,2,4-Triazol-3-ylsulfanylmethyl)-1,2,3-triazole derivatives. *ACS Omega, 6,* 301–316.

Azzam, K.A. (2023). SwissADME and pkCSM webservers predictors: An integrated online platform for accurate and comprehensive predictions for in silico ADME/T properties of artemisinin and its derivatives. *Complex Use of Mineral Resources*, *325*(2), 14-21.

Debela, D.T., Muzazu, S.G.Y., Heraro, K.D., Ndalama, M.T., Mesele, B.W., Haile, D.C., Kitui, S.K., & Manyazewal, T. (2021). New approaches and procedures for cancer treatment: Current perspectives. *SAGE Open Medicine, 9*, 1-10.

Dewar, M.J.S., Zoebisch, E.G., Healy, E.F., & Stewart, J.J.P. (1985). Development and use of quantum mechanical molecular models. 76. AM1: A new general purpose quantum mechanical molecular model. *Journal of American Chemical Society*, *107,* 3902–3909.

Cancer Chemoprevention Research Center (CCRC). (2009). Standard protocol for cytotoxicity assay using the MTT method. Universitas Gadjah Mada.

Eryanti, Y., Hendra, R., Herlina, T., Zamri, A., & Supratman, U. (2015). Synthesis of Curcumin analogue, N-H and *N*-benzil-4-piperidone and their cytotoxic activity. *Procedia Chemistry., 17,* 224–229.

Fathima, A.A., Kumaravel, V., Jonathan, D.R., Sadasivam, S.K., Yuvashri, R., & Usha, G.

(2024). Synthesis, structural examination, molecular interaction analysis, *in vitro* and *in silico* anticancer activity investigation of a new curcumin derivative: 1- (4 – chlorobenzoyl) - 3, 5 - bis ((E)-4-methoxybenzylidene) piperidin-4–one. *Chemical Physic Impact, 8*, 1-12.

Fikroh, R.A., Kimia, P., Tarbiyah, I., Keguruan, D., & Kalijaga, S. (2023). Synthesis of halogen substitued chalcone againts cervical cancer (hela) cell lines using green method. *Journal. Tropical Chemistry. Research and Education, 5,* 36–43.

Firdausy, A.F., Muti'ah, R., & Rahmawati, E.K. (2020). Predicting pharmacokinetic profiles of sunflowers's (*Helianthus annuus* L.) active compounds using *in silico* approach. *Journal of Islamic Medicine, 4,* 1–7.

Frisch, M.J., Trucks, G.W., Schlegel, H.B., Scuseria, G.E., Robb, M.A., Cheeseman, J. et al. (2016). Gaussian 09, Revision D.01. Gaussian, Inc.

Jamil, S.N.H., Ali, A.H., Feroz, S.R., Lam, S.D., Agustar, H.K., Mohd Abd Razak, M.R., & Latip, J. (2023). Curcumin and its derivatives as potential antimalarial and anti- inflammatory agents: A review on structure–activity relationship and mechanism of action. *Pharmaceuticals, 16,* 1-25.

Kaur, K., Al-Khazaleh, A.K., Bhuyan, D.J., Li, F., & Li, C.G. (2024). A review of recent curcumin analogues and their antioxidant, anti-inflammatory, and anticancer activities. *Antioxidants*, *13*(9), 1092.

Lipinski, C., Lombardo, F., Domini, P., & Feeney. (2001). Experimental and computational approaches to estimate solubility and permeability in drug discovery and development settings. *Advanced Drug Delivery Reviews,* 1-3.

Lohohola, P.O., Mbala, B.M., Bambi, S.M.N., Mawete, D.T., Matondo, A., & Mvondo, J.G.M. (2021). In silico ADME/T properties of quinine derivatives using SwissADME and pkCSM webservers. *International Journal of Tropical Disease and Health, 42*(11), 1-12.

Malki, A., Elbayaa, R.Y., Thabet, O.A., Sultan, A., & Youssef, A.M. (2017). Novel quinuclidinone derivatives induced apoptosis in human breast cancer via targeting p53. *Bioorganic Chemistry., 72,* 57–63.

Mustika, C.R., Astuti, E., & Mardjan, M.I.D. (2024). Molecular docking, synthesis and *in vitro* antiplasmodium assay of monoketone curcumin analogous from 2-chlorobenzaldehyde. *Indonesian Journal of Chemistry*, *24,* 638–651.

Muttaqin, F.Z., Ferdian Pratama, M., & Kurniawan, F. (2019). molecular docking and molecular dynamic studies of stilbene derivative compounds as sirtuin-3 (Sirt3) histone deacetylase inhibitor on melanoma skin cancer and their toxicities prediction. *Journal of Pharmacy, 2*(2). 112-121.

Oubahmane, M., Hdoufane, I., Delaite, C., Sayede, A., Cherqaoui, D., & El Allali, A. (2023). Design of potent inhibitors targeting the main protease of SARS-CoV-2 using QSAR modeling, molecular docking, and molecular dynamics simulations. *Pharmaceuticals*, *16*, 608.

Pourmadadi, M., Abbasi, P., Eshaghi, M.M., Bakhshi, A., Ezra Manicum, A.L., Rahdar, A., Pandey, S., Jadoun, S., & Díez-Pascual, A.M. (2022). Curcumin delivery and co-delivery based on nanomaterials as an effective approach for cancer therapy. *The Journal of Drug Delivery Science and Technology*, *78*, 1-17.

Pratama, M.R.F., Poerwono, H., & Siswodiharjo, S. (2020). ADMET properties of novel 5- O-benzoylpinostrobin derivatives. *Journal of Basic and Clinical Physiology and Pharmacology*, *30*, 1-13.

Radchenko, E.V, Dyabina, A.S., Palyulin, V.A., & Zefirov, N.S. (2016). Prediction of human intestinal absorption of drug compounds. *Russian Chemical Bulletin, International Edition*, *2*(65), 576-580.

Sancha, S.A.R., Szemerédi, N., Spengler, G., & Ferreira, M.J.U. (2023). Lycorine carbamate derivatives for reversing *p*-glycoprotein-mediated multidrug resistance in human colon adenocarcinoma cells. *International Journal of Molecular Sciences. 24*, 1-22.

Sohn, S.I., Priya, A., Balasubramaniam, B., Muthuramalingam, P., Sivasankar, C., Selvaraj, A., Valliammai, A., Jothi, R., & Pandian, S. (2021). Biomedical applications and bioavailability of curcumin—an updated overview. *Pharmacy*, *13*, 1-33.

Trott, O., & Olson, A.J. (2009). AutoDock Vina: Improving the speed and accuracy of docking with a new scoring function, efficient optimization, and multithreading. *Journal of Computational Chemistry, 31*, 455–461.

Wang, J. & Wu, S.G. (2023). Breast cancer: An overview of current therapeutic strategies, challenges, and perspectives, *Breast Cancer: Targets and Therapy*, *15*, 721–730.

Yang, Z.J., Huang, S.Y., Zhou, D.D., Xiong, R.G., Zhao, C.N., Fang, A.P., Zhang, Y.J., Li, H. Bin, & Zhu, H.L. (2022). Effects and mechanisms of curcumin for the prevention and management of cancers: An updated review. *Antioxidants*, *11(8)*,1-24.

Zelelew, D., Endale, M., Melaku, Y., Geremew, T., Eswaramoorthy, R., Tufa, L.T., Choi, Y., & Lee, J. (2023). Ultrasonic-assisted synthesis of heterocyclic curcumin analogs as antidiabetic, antibacterial, and antioxidant agents combined with in vitro and in silico studies. *Advances and Applications in Bioinformatics and Chemistry, 16*, 61–91.